The Astrophysical Journal, 692:1571–1581, 2009 February 20 doi:10.1088/0004-637X/692/2/1571

NONLINEAR DYNAMICS OF ACOUSTIC INSTABILITY IN A COSMIC RAY SHOCK PRECURSOR AND ITS IMPACT ON PARTICLE ACCELERATION

M. A. Malkov and P. H. Diamond
CASS and Department of Physics, University of California, San Diego, La Jolla, CA 92093, USA; mmalkov@ucsd.edu, phd@mamacass.ucsd.edu
Received 2008 August 27; accepted 2008 October 29; published 2009 February 24

ABSTRACT

An acoustic instability of a shock precursor driven by the pressure gradient of accelerated particles is studied in the nonlinear regime. The nonlinearity steepens unstable acoustic waves and turns them into shocks. The shocks form a "shocktrain" but they may merge into each other. Traveling wave solutions are obtained analytically in two different cases. In the first case, only acoustic instability is included and the characteristic scale (distance between the shocks) is limited only by the system size (while shocks merge). In the second case, the instability develops out of cyclotron unstable seed magnetohydrodynamic (MHD) waves. The spatial distance between the MHD wave packets sets the scale of the acoustic shocktrain. The internal structure of the individual shocks is presumably determined by the ion skin depth c/ω_{pi} and by the relaxation length of slightly superthermal particle distributions near these shocks. The shocks are assumed to be arbitrarily thin compared with the distance between them which is ensured by a small viscous term. Both types of solutions are dynamically verified by numerical calculations. The hydromagnetic flow in the shock precursor emerging from the acoustic instability is crucial for two recently suggested phenomena in diffusive shock acceleration. One phenomenon is the enhancement of the acceleration rate well above its standard (Bohm) value due to the narrowing of the shock precursor. The second phenomenon is the amplification of the long-scale magnetic field by an inverse cascade of Alfvén waves generated by accelerated particles and scattered in *k*-space on the acoustic perturbations.

Key words: acceleration of particles – cosmic rays – shock waves – supernova remnants – turbulence

1. INTRODUCTION

The concept of diffusive particle acceleration by strong shocks is based on a few simple ideas: (1) the energy source for acceleration is the *mechanical* shock energy; (2) particles tap this energy by alternately coupling to the downstream and upstream media (thus being virtually reflected by these converging media); (3) although the coupling process is essentially *magnetic*, the required magnetic field may remain dynamically unimportant. In other words, magnetic perturbations do not need to consume much of the shock energy to (elastically) scatter particles in the local fluid frame. Of course, the acceleration time is set by the strength of the magnetic field. Should the field be amplified in course of acceleration, the latter will proceed faster as the particles scatter more rapidly. However, if time is available, a mere *disturbance* of the ambient field (e.g., moderate Alfvén waves generated by the streaming particles) would suffice for the particles to consume much of the *mechanical* shock energy leaving the magnetic field to act only as a means of confining particles to the shock.

The above picture has the appeal of relative simplicity: (1) ambient magnetic field energy is negligible compared to the mechanical shock energy (magnetic Mach number $M_A \gg 1$) and remains such; (2) the available shock energy is distributed between only two main recipients: the energetic particles and the thermal plasma. However, even within this minimalistic model, the energy distribution (i.e., the *acceleration efficiency*) *critically* depends on a number of uncertain parameters. They include the injection rate of thermal particles as a function of the shock obliquity, the turbulent plasma heating rate in the cosmic ray (CR) shock precursor, and the transport characteristics of accelerated particles in this precursor. The acceleration efficiency not only depends sharply on these quantities, but it is even a multivalued function of them (Malkov 1997a, 1997b; Blasi et al. 2005) so that bifurcations occur.

Regardless of the difficulties of acceleration theory, the magnetic field amplification in young supernova remnants (SNRs) is likely to be an observational fact that needs to be addressed (Vink & Laming 2003; Berezhko & Völk 2004; Uchiyama et al. 2007; Aharonian et al. 2008). Most of the current field amplification models rely on the efficient particle (CRs) acceleration in that the amplification starts only when a significant fraction of shock energy is deposited into accelerated particles (Bell 2004; Vladimirov et al. 2006; Zirakashvili et al. 2008. Then, they drive one or a few available instabilities to generate a stronger field. Therefore, determining the acceleration efficiency within the above mentioned weak field approximation is a necessary step in understanding both the acceleration process and the subsequent magnetic field generation as its possible by-product and facilitator.

In this paper we consider an acoustic (the so-called Drury) instability (Drury & Falle 1986; Zank et al. 1990; Kang et al. 1992). The instability is driven by the pressure gradient of accelerated particles. Acoustic turbulence normally degenerates into shocks, so that there will be many (weaker) shocks ahead of the main flow discontinuity (subshock). Shocks will certainly alter the entire acceleration process. First, by even passively compressing the magnetic field (both ambient and turbulent) and thus creating *magnetic patterns*, the shocks modify particle transport. The latter becomes primarily nondiffusive, at least for particles of sufficiently high energy. Such change of particle transport and confinement dramatically changes the outcome of acceleration, i.e., the maximum particle energy, acceleration efficiency, and spectral index, as was demonstrated recently by these authors (Malkov & Diamond 2006). Second, the emerging acoustic flow scatters the Alfvén waves generated by accelerated particles in wavenumber space leading, in particular, to an inverse cascade (Diamond & Malkov 2007). Third, the heating rate of the thermal plasma also changes. Shock heating is more efficient than an oft assumed adiabatic heating or even turbulent heating by the Alfvén waves, particularly if the mechanical and CR energy dominate magnetic energy in the acceleration process. Finally, thermal particles are injected into acceleration at the newly created shocks in addition to the conventional subshock injection.

Now it follows that the shock waves upstream of the subshock are both a reflection and engine of acceleration. In the papers cited above the scattering field has been only prescribed as an ensemble of shock waves (shocktrain). The goal of this paper is to exactly determine the hydromagnetic flow structure in the shock precursor which is needed to calculate the acceleration parameters discussed above.

Shocktrains are frequently observed in situ upstream of cometary, interplanetary and even the Earth's bow shock. They are thought to be driven by unstable particle distributions, such as pick-up ions, ions reflected off the main shock, or those leaking from the downstream side of the shock. Note that in CR shock precursors, the CR pressure gradient is a powerful source of free energy to drive shocktrains.

The linear theory of acoustic and magnetoacoustic instabilities driven by the CR pressure gradient is well studied both in hydrodynamic and kinetic regimes (Drury & Falle 1986; Zank et al. 1990; Kang et al. 1992). The subsequent nonlinear steepening of these waves into shocks was also observed in simulations in the cited papers. The purpose of this paper is to develop a *nonlinear* theory describing the unstable wave growth, steepening, saturation, and interaction (merging) of the shocks to determine their strengths and the spatial pattern they form. As we stated, these are important characteristics of the magnetic turbulence of the CR precursor that are critical for both the acceleration theory (Malkov & Diamond 2006) and for the theory of magnetic field generation and spectral transfer (Diamond & Malkov 2007). In the latter theory, the MHD turbulence cascades to longer scales by scattering off the acoustic disturbances. This process was suggested to enhance acceleration and at the same time to avoid a rapid collisionless damping of the turbulent magnetic field, discussed earlier by Pohl et al. (2005). Finally, once these shocks can inject fresh particles into the acceleration throughout the precursor efficiently—as opposed to the community paradigm of the injection at the subshock—the models for diffusive particle acceleration should be modified. Therefore, the acoustic precursor instability has a strong impact on the acceleration efficiency, acceleration rate, spectral slope, and the maximum energy.

The plan of the paper is as follows. In the next section we derive a nonlinear evolution equation that describes generation of acoustic waves by Drury's instability and its subsequent saturation by nonlinear wave steepening that results in a shocktrain. In Section 3, we obtain traveling wave solutions of this equation. In Section 4, a solution is obtained for the case when Alfvén waves, driven by the cyclotron instability of the CRs, provide a seed perturbation for the Drury's instability. Numerical ramifications of these solutions that concern the shocktrain evolution and shock coalescence are presented in Section 5. We summarize and discuss the results in Section 6.

2. SHOCK PRECURSOR EQUILIBRIUM AND ITS STABILITY AGAINST GENERATION OF ACOUSTIC WAVES

In diffusive shock acceleration theory, the CR-modified shock precursor is an extended area ahead of a gaseous discontinuity (the latter is also called the subshock). The accelerated CRs diffuse into this area against the inflowing plasma, so that only the most energetic CRs with momenta $p \sim p_{\max}$ reach its end, Figure 1. The scale of this region is the largest in the problem (apart from the shock geometry related scales, such as the radius of a blast wave, etc.) and can be estimated as $L_{\rm dif} \simeq \kappa(p_{\max})/U_1$, where κ is the momentum-dependent particle diffusivity and U_1 is the plasma speed far upstream. Along with $L_{\rm dif}$, we introduce the flow modification length (or modified shock precursor length) $L_p \simeq \kappa(p_*)/U_1 \leqslant L_{\rm dif}$. Here p_* is the particle momentum which makes the maximum contribution to the CR pressure. The momentum p_* can be equal to $p_{\max}$ (when in a nonlinear regime the spectrum is so flat that the pressure diverges with p). It is also possible that $p_* \ll p_{\max}$, in which case the spectrum develops a break at p_* and continues to $p_{\max}$ with a steeper, pressure converging slope (Malkov & Diamond 2006). Particles with $p > p_*$ do not modify the flow significantly in the region $L_p < x < L_{\rm dif}$.

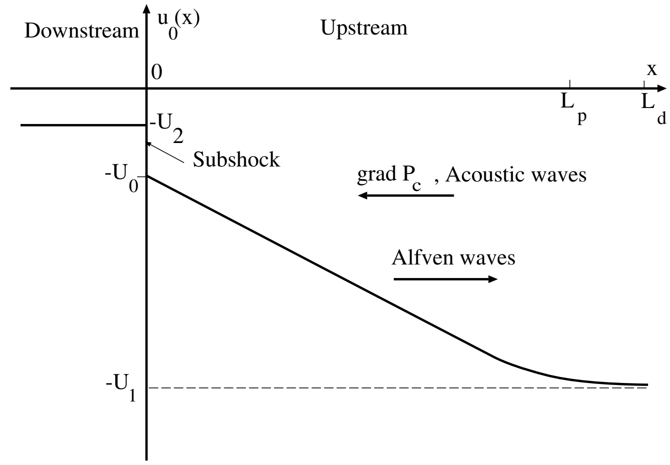

Figure 1. Typical velocity profile $u_0(x)$ of a plasma flowing into a modified shock, shown in the subshock frame. The CR pressure gradient in the shock precursor drives both Alfvén waves propagating in the upstream direction and acoustic waves propagating toward the subshock.

The pressure of CRs makes work against the flow and gradually slows it down within the CR precursor. This occurs through the generation of MHD waves by the same pressure gradient of CRs (or equivalently, by their pitch angle anisotropy) and through the ponderomotive pressure that these waves exert on the incoming plasma (Achterberg 1981). The ponderomotive pressure, however, does not need to be as high as the flow ram pressure to slow down the flow. In fact, the CR pressure decelerates the flow by entering the total pressure balance and compensating the plasma current in Ampere's law allowing thus even weak magnetic field perturbations to decelerate the flow (Blandford & Funk 2007). Likewise, the MHD waves that scatter CRs in course of acceleration do not need to reach an energy comparable with the CR total energy since the scattering is elastic in the local wave frame (and the latter is close to the local fluid frame).

We also anticipate strong heating of the precursor plasma because of the acoustic turbulence. Therefore, we do not assume the plasma to be heated adiabatically and treat its equilibrium temperature as an arbitrary function of coordinate. The temperature is maintained by the acoustic turbulence. However, we defer the study of turbulent heating to a future paper. In this paper, as we stated already, we assume that the mechanical and CR energy dominate the magnetic and thermal energy, even though the magnetic field may be amplified and plasma may be heated significantly due to hydrodynamic turbulence resulting from the acoustic or other instabilities.

In the simplest one-dimensional form the equations for the gas flow read

$$\frac{\partial \rho}{\partial t} + \frac{\partial}{\partial x}\rho u = 0 \tag{1}$$

$$\frac{\partial u}{\partial t} + u\frac{\partial u}{\partial x} = -\frac{1}{\rho}\frac{\partial}{\partial x}\left(P_c + P_g\right) + 2\mu\frac{\partial^2 u}{\partial x^2}. \tag{2}$$

Here ρ, u, and P_g denote the mass density, velocity and thermal pressure of the plasma, respectively. As we stated earlier, P_g is considered to be a given function of x. The last term on the right-hand side (rhs) of Equation (2) represents an anomalous viscosity due to microinstabilities that are likely to occur in the regions of strong velocity variations. In particular, these instabilities can be driven by shock reflected particles as well by hot particles that leak from downstream. These instabilities have been extensively studied in regard to collisionless shock physics (Sagdeev 1979; Kennel et al. 1985; Papadopoulos 1985). To close the system of Equations (1) and (2), we will determine the CR pressure P_c in Equation (2) from the convection–diffusion equation for the pitch angle averaged distribution function of accelerated particles

$$\frac{\partial f}{\partial t} + u\frac{\partial f}{\partial x} - \kappa(p)\frac{\partial^2 f}{\partial x^2} = \frac{p}{3}\frac{\partial u}{\partial x}\frac{\partial f}{\partial p}. \tag{3}$$

Here, the CR pressure is given by

$$P_c = \frac{4\pi}{3}mc^2\int \frac{p^4}{\sqrt{1+p^2}} f\,dp \tag{4}$$

and the particle momentum p is normalized to mc, where m is the proton mass. We assume for simplicity that the particle diffusion coefficient depends only on momentum and ignore its spatial variations. A few comments are in order here. First, in a simple but maybe not totally unrealistic case of $\kappa(p,x) = \kappa_1(p)\kappa_2(x)$, the x-dependence of κ can be removed by a coordinate transformation. Second, in terms of the acoustic instability studied further in this paper, the dependence of κ on other variables (such as ρ; Drury & Falle 1986) yields a simple factor in a final expression for the growth rate $\gamma \propto (1 + \partial \ln\kappa/\partial \ln\rho)$ which we de facto ignore and replace by unity. There are no strong arguments for the case $1 + \partial \ln\kappa/\partial \ln\rho \approx 0$. Moreover, the acoustic turbulence that results from this instability primarily changes the regime of particle transport, rendering the transport nondiffusive in at least the most interesting, high energy region (Malkov & Diamond 2006). This explains our choice of κ as a simple growing function of momentum. We believe that this is the only reasonable (but important!) physical assumption to make, based on our current understanding (or ignorance) of the particle transport in turbulent shock precursors.

2.1. *Weakly Nonlinear Acoustic Waves in a CR Precursor*

We start from the standard equilibrium solution of Equations (1) and (2) in the shock precursor, $x > 0$ (Figure 1):

$$\rho_0(x)\,u_0(x) = J = \text{const} \tag{5}$$

$$\rho_0 u_0^2 + P_{g0}(x) + P_{c0}(x) = \text{const}. \tag{6}$$

Here, the 0-indexed variables denote the equilibrium distributions of the quantities introduced earlier in Equations (1) and (2). Since the flow is highly supersonic, the unstable acoustic waves are convected much faster than they propagate in the local fluid frame, suggesting the following Lagrangian coordinate:

$$d\xi = dx - u_0(x)\,dt. \tag{7}$$

Note that in the new variables ξ, t the stationary parts of the velocity and density profiles depend on time. The dependence is slow compared with the timescale of acoustic perturbations if $kL_p/M_s \gg 1$, where k is a typical wavenumber of the sound waves and $M_s = u_0/c_s$ is the local Mach number of the flow. Expanding Equations (1) and (2) in small but finite deviations of the density and velocity from their equilibrium quantities,

$$\tilde{\rho} = \rho - \rho_0 \ll \rho_0, \quad \tilde{u} = u - u_0 \ll u_0, \tag{8}$$

yields the following equations for the perturbations

$$\frac{\partial \tilde{\rho}}{\partial t} + \rho_0\frac{\partial \tilde{u}}{\partial \xi} + \frac{\partial}{\partial \xi}\tilde{\rho}\tilde{u} = 0, \tag{9}$$

$$\frac{\partial \tilde{u}}{\partial t} + \tilde{u}\frac{\partial \tilde{u}}{\partial \xi} = \frac{\tilde{\rho}}{\rho_0^2}\frac{\partial}{\partial \xi}\bar{P}_{tot} - \frac{1}{\rho_0}\left(1 - \frac{\tilde{\rho}}{\rho_0}\right)\frac{\partial}{\partial \xi}\left(\tilde{P}_g + \tilde{P}_c\right) + 2\mu\frac{\partial^2 \tilde{u}}{\partial \xi^2}. \tag{10}$$

Here, we have introduced the average total pressure

$$\bar{P}_{\text{tot}} = P_{g0} + P_{c0} \simeq \bar{P}_c$$

and the oscillating parts of the gas and CR pressure

$$\tilde{P}_g = P_g - \bar{P}_g,$$

$$\tilde{P}_c = P_c - \bar{P}_c.$$

The gas pressure perturbations can be expressed through the density perturbations in the usual way (Landau & Lifshitz 1987),

$$\tilde{P}_g = c_s^2\tilde{\rho}\left(1 + \frac{\gamma_g - 1}{2\rho_0}\tilde{\rho}\right), \tag{11}$$

where $\gamma_g = 5/3$ is the adiabatic gas index. We shall follow a procedure which is very similar to the standard gas dynamics derivation of the Burgers equation, except for the extra terms with the CR pressure. Not surprisingly, we will arrive at the Burgers equation supplemented with such extra terms. It is convenient to reduce Equations (9) and (10) by differentiating first Equation (9) with respect to t and by using then Equation (10). The following equation results:

$$\left(\frac{\partial}{\partial t} - c_s\frac{\partial}{\partial \xi}\right)\left(\frac{\partial}{\partial t} + c_s\frac{\partial}{\partial \xi}\right)\tilde{\rho} = -\frac{1}{\rho_0}\frac{\partial \bar{P}_c}{\partial \xi}\frac{\partial \tilde{\rho}}{\partial \xi} + \frac{\partial^2 \tilde{P}_c}{\partial \xi^2} + c_s^2\frac{\gamma_g - 2}{2\rho_0}\frac{\partial^2 \tilde{\rho}^2}{\partial \xi^2} - \frac{\partial}{\partial \xi}\left(2\tilde{u}\frac{\partial \tilde{\rho}}{\partial t} + \tilde{\rho}\frac{\partial \tilde{u}}{\partial t}\right) - 2\mu\rho_0\frac{\partial^3 \tilde{u}}{\partial \xi^3}. \tag{12}$$

The terms on the lhs describe forward and backward propagating waves, of which the backward wave, $\tilde{\rho} \approx \tilde{\rho}(\xi + c_s t)$, is unstable due to the first term on the rhs. The role of the second term on the rhs will be clarified later. Here, we simplify the last equation assuming the backward propagating (unstably growing) waves to dominate, which means that

$$\frac{\partial \tilde{\rho}}{\partial t} \approx c_s \frac{\partial \tilde{\rho}}{\partial \xi}.$$

Using the last relation, Equation (12) can be integrated by ξ. In addition, the velocity perturbation $\tilde{u}$ can be expressed through the density perturbations $\tilde{\rho}$ from Equation (9) as follows

$$\tilde{u} \approx -\frac{c_s}{\rho_0}\tilde{\rho}. \tag{13}$$

Equation (12) can, in turn, be transformed to the following, modified Burgers equation

$$\frac{\partial \tilde{\rho}}{\partial t} - c_s \frac{\partial \tilde{\rho}}{\partial \xi} - \frac{\gamma_g + 1}{2\rho_0} c_s \tilde{\rho} \frac{\partial \tilde{\rho}}{\partial \xi} - \mu \frac{\partial^2 \tilde{\rho}}{\partial \xi^2} = \frac{1}{2c_s}\left(\frac{\partial \tilde{P}_c}{\partial \xi} - \frac{\tilde{\rho}}{\rho_0}\frac{\partial \bar{P}_c}{\partial \xi}\right). \tag{14}$$

The lhs of this equation is the familiar Burgers part, whereas the effect of the CR pressure is on its rhs. The first term in parentheses is the response of CR to the density fluctuations of the plasma, $\tilde{\rho}$, which we provide in the next subsection. The second term is actually the Drury's instability driving term related to the averaged CR pressure gradient which is considered here to be a known quantity. Therefore, to close the above equation, we need to calculate the CR response to the acoustic fluctuations. This will be done in the next subsection and in the Appendix.

2.2. *CR Response to Acoustic Perturbations*

Usually, CRs respond to acoustic perturbations dissipatively because of their fast diffusion. The response was first calculated by Ptuskin (1981) within the MHD approach. In Drury's instability context the CR response was calculated by a number of authors starting from Drury & Falle (1986) (see, e.g., Zank et al. 1993 and references therein). The main guidance from these works is that the short sound waves decouple from CRs, so that the latter can be largely ignored in Equation (14) apart from the destabilizing contribution from their background gradient. However, given the above assumption about strong momentum dependence of the CR diffusivity, we need to confirm this assertion using a kinetic approach. In principle, such calculations are also available in the literature (see e.g., Zank et al. 1993 and a very recent one by Finazzi & Vietri 2008). Unfortunately, they arrived at contradictory conclusions (even though the assumptions are similar) in that the first paper claims that CRs can destabilize the acoustic waves (squeezing instability), whereas the authors of the second paper arrive at the opposite conclusion (apparently unaware of the first paper). More importantly, both papers do not consider Drury's instability, i.e., the CR background pressure gradient is not included. Therefore, their results cannot be utilized here directly.

A somewhat superficial examination of the above controversy suggests that it originates in part from the different choices of the CR background distribution functions. More importantly, perhaps, they also treat the transition in the momentum space between the thermal and energetic particles in different ways. Therefore, to calculate the CR response, it is best to proceed from an equilibrium solution of the CR distribution function in the CR precursor. Such a solution has been found as an expansion in $1/\kappa(p)$ series by Malkov (1997a) specifically for the case of rapidly increasing $\kappa(p)$. It is *critical* that κ grows faster than $p^{1/2}$. In a short wave, adiabatic limit, i.e., when $k\kappa \gg c_s$, we can neglect the time derivative term in Equation (3) (here, we have used an estimate for the frequency $\omega - ku_0 \simeq kc_s$). It is also convenient to use a flow potential ϕ, defined as $u = \partial\phi/\partial x$, instead of u. Thus, instead of Equaxtion (3) we write

$$\frac{\partial \phi}{\partial x}\frac{\partial f}{\partial x} - \kappa(p)\frac{\partial^2 f}{\partial x^2} = \frac{p}{3}\frac{\partial^2 \phi}{\partial x^2}\frac{\partial f}{\partial p}. \tag{15}$$

One can generate a solution in a series of ϕ/κ which can be represented formally as (Malkov 1997a)

$$f = f_0(p)\exp\left[\frac{q(p)}{3\kappa(p)}\phi(x)\right], \qquad x \geqslant 0, \tag{16}$$

where f_0 is a (so far) arbitrary function of momentum and

$$q = -\frac{\partial \ln f_0}{\partial \ln p}$$

is the spectral index. The procedure of summation of the series in $|\phi/\kappa| \ll 1$ to yield the sum given by Equation (16) is not rigorous, which probably explains why the entire approach is dubbed "semianalytic." Nevertheless, the result, i.e., the solution in Equation (16), satisfies Equation (15) *exactly* (for arbitrary ϕ/κ) as long as the flow profile $\phi(x)$ is specified properly. Of course, the latter *must* be specified to satisfy the pressure balance, given by Equation (6). In fact the flow profile, initially chosen to make the solution in Equation (16) an exact solution of Equation (15), turns out to satisfy the pressure balance condition, Equation (6). More precisely, Equation (6) is strictly satisfied within the shock precursor, i.e., for $x < L_p$, $M_s \gg 1$, and for $p_{\max}/p_{\rm inj} \gg 1$, where $p_{\rm inj}$ is the injection momentum. Therefore, the solution given by Equation (16) is an equilibrium solution of the system given by Equations (1)–(4). This solution, however, becomes somewhat inaccurate at the boundary of the shock precursor, i.e., for $x \gtrsim L_p$. On the other hand, $\partial^2\phi/\partial x^2 \to 0$, so that $u(x) \simeq$ const there, and the solution in Equation (6) is obvious. It can be obtained from Equation (16) by a formal choice of $q = 3$. *Within the precursor*, q turns out to be close to $q = 3\frac{1}{2}$, so that the correction to be made while continuing the internal solution to the periphery of the CR precursor is not very significant. Of course, to construct a regular (uniformly valid) asymptotic expansion for the CR shock structure with a self-consistent particle spectrum, this correction is required. It can be made by matching the internal solution described above to a perturbative, outer solution (for $P_c(x)/\rho u^2 \ll 1$), applicable in the area $x \gtrsim L_p$, found earlier by Blandford (1980). At the same time, both the internal solution for f, Equation (16), and a corresponding self-consistent flow profile, $u_0(x)$, exponentially approach their proper asymptotic limits as $x \to \infty$ ($f \to 0$ and $u_0 \to -U_1$) without any matching with an outer solution. Therefore, the matching would not change the internal solution for f or for $u_0(x)$ found in Malkov (1997a) because the corrections to these quantities at the edge of the precursor are exponentially small. This explains why the agreement with the numerical solution is almost perfect (Moskalenko et al. 2007), despite the minor shortcomings of the asymptotic expansion described above.

Therefore, for the purposes of the present paper the internal solution alone is sufficient. Moreover, the acoustic instability develops in the area of high CR pressure, i.e., for $x < L_p$. The background flow stationarity and a sufficiently steep $\kappa(p)$ dependence are thus the only restrictions imposed. Therefore, we can apply this solution also to a flow that is perturbed by sound waves, provided that the condition $k\kappa(p) \gg c_s$ is met. Clearly, this is a very mild restriction on the valid range of momenta p since the condition $k > L_p^{-1} = U_1/\kappa(p_*)$ must be valid in any event, so that it is sufficient to require $\kappa(p)/\kappa(p_*) \gtrsim M_s^{-1}$. For Bohm diffusion the last inequality simplifies to $p/p_* \gtrsim M_s^{-1}$. In fact, this condition is automatically fulfilled throughout the CR precursor except for low-energy particles that are close to the subshock. Indeed, let us substitute

$$\phi(x) = \phi_0(x) + \tilde{\phi}(x,t) \tag{17}$$

into Equation (16) with ϕ_0 being the steady background flow potential ($u_0 = \partial\phi_0/\partial x$) and $\tilde{\phi}$ its perturbation. Thus,

$$f = F_0(p,x)\exp\left[\frac{q}{3\kappa(p)}\tilde{\phi}\right]. \tag{18}$$

The unperturbed part of the distribution function

$$F_0 = f_0(p)\exp\left[\frac{q}{3\kappa(p)}\phi_0(x)\right] \tag{19}$$

cuts off exponentially for particle momenta $p < p_{\min}$, where $p_{\min}(x)$ can be determined as $\kappa(p_{\min}) = q(p_{\min})\phi_0(x)/3$. For Bohm diffusion, the smallest gyroradius that particles can have for a given x is $r_g(p_{\min}) \simeq qxU_0/c$. Therefore, the stationarity requirement can be easily fulfilled for all particle momenta p, as long as $x/L_p \gtrsim U_1/U_0 M_s$.

Now that the particle distribution is available, we can calculate the CR response in Equation (14) as follows:

$$\tilde{P}_c = \frac{4\pi}{3}mc^2\int_0^\infty \frac{p^4 dp}{\sqrt{1+p^2}}F_0(p,x)\left\{\exp\left[\frac{q}{3\kappa(p)}\tilde{\phi}\right]-1\right\}. \tag{20}$$

Note that, according to the background solution F_0, the integration limits here should be $p_{\rm inj}$ and $p_{\max}$ instead of 0 and ∞ since the contribution of F_0 to P_c diverges with $p_{\max}$ ($F_0 \propto p^{-7/2}$, as $p \to \infty$) and must be cut off. The *perturbation* of P_c, however, i.e., $\tilde{P}_c$, *converges* even without imposing a cut off on F_0 at the upper limit because of the condition $\kappa(p) > Cp^{1/2}$ (where $C = $ const) and the factor in the braces in Equation (20). At the lower integration limit, the pressure integral also cuts off by itself, as we discussed above. Therefore, we extended the integration to the entire momentum space.

Let us write the particle diffusivity κ for Bohm diffusion as

$$\kappa(p) = \kappa_*\frac{p^2}{p_*\sqrt{1+p^2}}, \tag{21}$$

where $p_* \gg 1$ is some fiducial momentum which we take to be equal to the maximum of the background particle partial pressure contribution and $\kappa_* = \kappa(p_*)$. Assuming $\tilde{\phi}/\kappa(p_{\min}) \lesssim 1$, from Equation (20) we obtain the linear response of the CR particles to the acoustic perturbations that are characterized by the flow potential $\tilde{\phi}$:

$$\tilde{P}_c \simeq \frac{4\pi}{9}\frac{mc^2 p_*}{\kappa_*}\tilde{\phi}\int_0^\infty qp^2F_0(p,x)\,dp = \frac{\bar{q}}{9}\frac{mc^2p_*}{\kappa_*}n_c(x)\tilde{\phi}, \tag{22}$$

where we introduced the CR number density

$$n_c = 4\pi\int_0^\infty p^2F_0(p,x)\,dp \tag{23}$$

and where $\bar{q}$ is the value of $q(p)$ averaged over the particle spectrum $F_0(p)$. In a strongly nonlinear acceleration regime the index $q(p)$ continuously decreases with p, starting from $q = 3r_s/(r_s-1) \geqslant 4$ at $p = p_{\rm inj}$ (with r_s being the subshock strength), then the index approaches the value $q = 4$ in the momentum range $p_{\rm inj} < p < 1$, then it decreases even more, to $q = 3\frac{1}{2}$ for $1 < p < p_{\max}$. Finally, the index q ends up at the cut off $p_{\max}$ with its value $q = 3\frac{1}{4}$ (Malkov 1997a). The latter feature results from the assumption about an abrupt cut off. The above $q(p)$ behavior perfectly reproduces the results of Monte Carlo simulations (Ellison et al. 2000) in the entire $p_{\rm inj} < p < p_{\max}$ range, when they are made under the same assumptions (see Moskalenko et al. 2007 for the comparison of analytic and numerical results).

Using Equations (13) and (22) we can rewrite Equation (14) as follows

$$\frac{\partial\tilde{\rho}}{\partial t} - c_s\frac{\partial\tilde{\rho}}{\partial\xi} - \frac{\gamma_g+1}{2\rho_0}c_s\tilde{\rho}\frac{\partial\tilde{\rho}}{\partial\xi} - \mu\frac{\partial^2\tilde{\rho}}{\partial\xi^2} = \gamma\tilde{\rho}, \tag{24}$$

where the acoustic instability growth rate is

$$\gamma = -\frac{1}{2\rho_0 c_s}\frac{\partial\bar{P}_c}{\partial\xi} - \frac{\bar{q}}{18}\frac{mc^2p_*}{\kappa_*}\frac{n_c(x)}{\rho_0}. \tag{25}$$

The first term on the rhs represents the instability growth rate (positive for the chosen negative direction of wave propagation) found by Drury & Falle (1986). The second term is the background CR response to the acoustic waves which is always stabilizing. One can rewrite the second term as

$$\gamma_{\rm damp} \simeq -\frac{\bar{q}}{6}\frac{\bar{P}_c}{\kappa_*\rho_0}. \tag{26}$$

Apart from the factor $\bar{q}/3 \approx 7/6$ instead of $\gamma_c \approx 4/3$ (adiabatic index of the CR gas), the damping term also coincides with that found by Drury & Falle (1986). This minor difference is due to the two-fluid treatment in the cited paper, for which $n_c = 0$ but $\bar{P}_c > 0$. Therefore, the transition to $P_c \propto p_* n_c > 0$ (implying an infinite p_*) depends on the CR spectrum which the two-fluid model cannot handle, and which is reflected in the factor $\bar{q}$ (see Malkov & Drury 2001 for a general discussion of the kinetic versus two-fluid treatment of CRs). Of course, one may replace q in Equation (22) by $-\partial\ln F_0/\partial\ln p$ instead of $-\partial\ln f_0/\partial\ln p$, integrate by parts, and reach thus a formal agreement between the two approaches. In both cases, however, $\gamma_{\rm damp} \sim \gamma/M_s \ll \gamma$ and can be neglected.

3. TRAVELING WAVE SOLUTION DRIVEN BY ACOUSTIC INSTABILITY

It is best to start the analysis of Equation (24) from the simplest case of a periodic traveling wave solution. The reasons for that are the following. First, traveling wave solutions are, in general, very strong attractors of an externally or unstably driven Burgers equation (Malkov et al. 1995). In the CR shock precursor, the highest energy particles, upon diffusing to the outermost part of it, excite MHD waves via the cyclotron instability. The typical wavelength of these waves is of the order of the particle Larmor radius and they should also contain a compressible component of the same length (Kotelnikov et al. 1991). Even though the resonance condition allows an excitation of shorter waves by particles with the same energy but moving at larger pitch angles, a widely accepted resonance sharpening procedure (Skilling 1975) suggests that the dominant wavenumber is $k_0 \sim r_g(p_*)$. Now that Drury's instability develops while these waves are convected through the precursor, we can consider them as seed waves for the instability. Note that the shorter seed waves in the spectrum can be ignored also because of a fast short wave generation by steepening of the longest waves via the strong quadratic nonlinearity in Equation (24). In addition, shocks emerged out of the short scales merge quickly or are absorbed by stronger shocks which originate from longer scales. However, the effect of the width of the initial spectrum plays an important part in the dynamics of the unstably driven Burgers equation. The dynamics will be studied in more detail in Sections 3 and 4.

Turning to the traveling wave solution, it is convenient to rewrite Equation (24) in the following form (after transforming to the system moving at the speed c_s, i.e., after introducing a new coordinate $\zeta = \xi + c_s t$)

$$\frac{\partial \hat{\rho}}{\partial t} + \hat{\rho}\frac{\partial \hat{\rho}}{\partial \zeta} = \gamma \hat{\rho} + \mu \frac{\partial^2 \hat{\rho}}{\partial \zeta^2}. \qquad (27)$$

Here, we have normalized the density perturbations by introducing $\hat{\rho} = \left(\gamma_g + 1\right) c_s \tilde{\rho}/2\rho_0$. We shall look for a periodic traveling wave solution of the form $\hat{\rho} = \hat{\rho}(\zeta - Ct)$ that also satisfies the condition $\langle\hat{\rho}\rangle = 0$, where $\langle\cdot\rangle$ denotes a period averaged quantity. The simplest family of such solutions can be obtained in the case $C = 0$, which will be numerically confirmed in Section 5 to be an attractor of the complete time-dependent system given by Equation (27). For this simplest case we obtain the following ordinary differential equation for $\hat{\rho}$:

$$\hat{\rho}\frac{\partial \hat{\rho}}{\partial \zeta} = \gamma \hat{\rho} + \mu \frac{\partial^2 \hat{\rho}}{\partial \zeta^2}. \qquad (28)$$

Integrating this equation yields the following relation between $\hat{\rho}$ and $\partial\hat{\rho}/\partial\zeta$

$$\frac{\hat{\rho}^2}{2\mu} - \frac{\partial \hat{\rho}}{\partial \zeta} - \gamma \ln\left(1 - \frac{1}{\gamma}\frac{\partial \hat{\rho}}{\partial \zeta}\right) = E = \text{const}. \qquad (29)$$

The last result describes a family of traveling wave solutions labeled by the amplitude parameter E, Figure 2. This parameter is related to the wave amplitude as follows:

$$\hat{\rho}_{\max} = -\hat{\rho}_{\min} = \sqrt{2\mu E}.$$

In the limit of small $\hat{\rho}$ the system is identical to a linear oscillator. In this case from Equation (29) we have

$$\frac{1}{2\gamma}\left(\frac{\partial \hat{\rho}}{\partial \zeta}\right)^2 + \frac{\hat{\rho}^2}{2\mu} = E. \qquad (30)$$

The last relation is equivalent to the energy integral of a linear oscillator of mass $1/\gamma$ and of elastic constant $1/\mu$. The coordinate of the oscillator is $\hat{\rho}$ and the role of time is played by ζ. The oscillator frequency (in our case the spatial period) is independent of its energy. In this limit, the solution for $\hat{\rho}$ clearly describes a linear acoustic wave that propagates at the sound

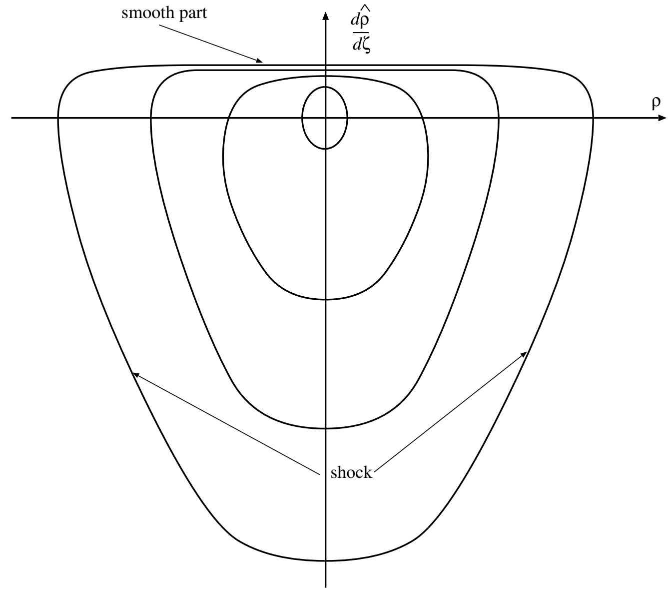

Figure 2. Phase portrait for Equation (29). Several trajectories are shown for different values of the constant E. The horizontal portions of the orbits correspond to the smooth part of the solution, where $\partial\hat{\rho}/\partial\zeta \approx \gamma$, while the bottom part of each orbit relates to the shock transition.

speed c_s. The viscous damping is compensated in this case by the instability (innermost contour in Figure 2). In a general, nonlinear case we obtain the following relation between the wave period and its amplitude, i.e., the nonlinear dispersion relation

$$L = \oint \frac{d\hat{\rho}}{\left(\partial\hat{\rho}/\partial\zeta\right)} = \sqrt{\frac{\mu}{2}} \oint \frac{d\psi}{(\gamma - \psi)\sqrt{E + \psi + \gamma \ln(1 - \psi/\gamma)}}, \qquad (31)$$

where we have used $\psi = \partial\hat{\rho}/\partial\zeta$ as an integration variable. As usual, the integral is to be taken between the roots of the radical along the closed trajectory of the "oscillator." The above traveling wave solution of the unstable Burgers equation is exact, but it will be useful to have simplified versions of the solution in the two limiting cases discussed above. The small amplitude solution that corresponds to the condition $\psi \ll \gamma$ is characterized by the first integral already given by Equation (30) and by the amplitude-independent wave period

$$L \simeq \frac{1}{\gamma}\sqrt{\frac{\mu}{2}} \oint \frac{d\psi}{\sqrt{E - \psi^2/2\gamma}} = 2\pi\sqrt{\frac{\mu}{\gamma}}. \qquad (32)$$

Of course, this result can be obtained easily by retaining only the instability and the viscous terms in Equation (27). An opposite, strongly nonlinear regime is more interesting to the present study. In this case the maximum value of ψ approaches γ and we obtain from Equation (31) the following relation between the wave amplitude, $\sqrt{2\mu E}$ and the wave period L:

$$L = \sqrt{\frac{\mu}{2\gamma}} \oint \frac{d\vartheta}{\sqrt{E/\gamma + 1 + \vartheta - \exp(\vartheta)}}$$
$$\simeq 2\sqrt{\frac{\mu}{2\gamma}} \int_{-\frac{E}{\gamma}}^{0} \frac{d\vartheta}{\sqrt{E/\gamma + \vartheta}} = \frac{4}{\gamma}\sqrt{\mu E/2} = \frac{2\hat{\rho}_{\max}}{\gamma}, \qquad (33)$$

where we have used the substitution $\vartheta = \ln(1 - \psi/\gamma)$. The last relation can also be easily obtained directly from Equation (27) by equilibrating the nonlinearity and the driving terms so that the solution becomes piecewise linear:

$$\hat{\rho} = \gamma x, \quad -L/2 < x < L/2 \pmod{L}. \tag{34}$$

Here $\hat{\rho}$ runs between $-\hat{\rho}_{\max}$ and $\hat{\rho}_{\max}$. At the points $x = (n + 1/2)\,L$ (with integral n) shocks are to be placed, where $\hat{\rho}$ returns from $\hat{\rho}_{\max}$ to $-\hat{\rho}_{\max}$. The spatial structure of the shock transition can be obtained from the exact formula given by Equation (29) upon neglecting the logarithm term:

$$\frac{\hat{\rho}^2}{2\mu} - \frac{\partial\hat{\rho}}{\partial\zeta} = \frac{\hat{\rho}^2_{\max}}{2\mu}. \tag{35}$$

A conventional shock transition then follows from the last formula:

$$\hat{\rho} = -\hat{\rho}_{\max}\tanh\left[\frac{\hat{\rho}_{\max}}{2\mu}\left(\zeta - \frac{L}{2}\right)\right], \quad \pmod{L}. \tag{36}$$

A smooth connection of this shock profile with the linear portion of the solution above can be obtained by matched asymptotic expansion or multiscale methods. This type of solution is known as a shocktrain solution which occurs in many driven nonlinear evolution equations. Shocktrains form when the driven waves grow and steepen into shocks. The overall solution consists then of extended regions where the nonlinearity is balanced by the driver. These regions are interspersed by shocks, where the nonlinearity is balanced by the dissipation (and dispersion, if present). These types of solutions are shown to be very persistent; they can be periodic or even spatially chaotic. They can be stationary or evolve in time depending on the parameters (see Malkov 1996 and references therein for details).

4. TRAVELING WAVE SOLUTION DRIVEN BY ACOUSTIC AND CYCLOTRON INSTABILITIES

As we noted earlier, MHD waves are driven throughout the shock precursor by a slightly anisotropic CR distribution. Even though these waves may be created incompressible (since Alfvén waves propagating along the field line grow at the highest rate), they can efficiently convert into magnetoacoustic, i.e., compressible, waves (e.g., Kotelnikov et al. 1991). The compressible perturbations undergo the acoustic instability and we include them into the Burgers equation, Equation (27), as a driver:

$$\frac{\partial\hat{\rho}}{\partial t} + \hat{\rho}\frac{\partial\hat{\rho}}{\partial\zeta} - \gamma\hat{\rho} - \mu\frac{\partial^2\hat{\rho}}{\partial\zeta^2} = Q\,(\zeta - vt). \tag{37}$$

Here Q is the source of the density perturbations originated by the cyclotron instability. Since Equation (37) is written in a reference frame that moves toward the subshock at speed c_s, and the Alfvén waves propagate in the local fluid frame away from the subshock at speed v_A, the speed at which the source moves is $v = c_s + v_A$. This speed enters the argument of the driver Q. It is now convenient to transform to the driver frame, so that the last equation can be rewritten as

$$\frac{\partial U}{\partial t} + U\frac{\partial U}{\partial y} - \gamma\,(U + v) - \mu\frac{\partial^2 U}{\partial y^2} = Q\,(y), \tag{38}$$

where we have denoted $U = \hat{\rho} - v = \hat{\rho} - c_s - v_A$ and $y = \zeta - vt$. Note that the speed $v = c_s + v_A$ is the mean value of U.

To connect solutions of this equation with the numerical studies of Equations (27) and (38) in the next section, we assume that an acoustic perturbation source Q is a superposition of a few linear acoustic modes resulting from conversion of Alfvén, or slightly oblique magnetosonic waves. These waves are excited by the cyclotron instability of accelerated particles. We select a few modes with wavenumbers $k_n \sim k_A$ separated by $k_{n+1} - k_n = \Delta k$, where k_A is a typical wavenumber in the wave packet. It can be estimated as $k_A \sim 1/r_L$, where r_L is a typical Larmor radius of CRs that drive the cyclotron instability. The resulting wave field is therefore a periodic sequence of packets separated in space by $L = 2\pi/\Delta k$ which will be the total period of the solution. The spatial size of each packet is about $L_{\rm wp} = 2\pi/N_{\rm mod}\Delta k$, where $N_{\rm mod}$ is the total number of modes in the packet. Note that nearby the subshock the spectrum of excited Alfvén waves is broad, as particles with all momenta from $p_{\rm inj}$ to $p_{\max}$ are present, while the spectrum is narrower at the periphery of the precursor, since only the highest energy particles can reach it. In addition, the width of a packet depends on the wave conversion mechanisms. Notwithstanding these uncertainties, we take a moderate number of acoustic mode perturbations in Equation (38) though this number is large enough to separate the periodic sequence of packets by a distance which is long enough to approximate $Q \simeq 0$ in the space between the packets. Therefore, we can represent Q as $Q\,(y/\epsilon)$ where ϵ is a small parameter, characterizing the width of each packet in the shocktrain, compared with the distance between the packets, i.e., $\epsilon = 1/N_{\rm mod}$ and $Q\,(y \gg 1) \approx 0$. Now we can construct a solution within each period of the driver, similar to the solution obtained in the last section for the case of $Q = 0$. Here, however, the period of the solution is *prescribed* by the period of Q.

Let us denote $z = y/\epsilon$, $V = U/\sqrt{\epsilon}$ and look for a traveling wave solution of Equation (38) (which is simply a steady state solution in the driver's reference frame). The equation takes the following form:

$$V\frac{\partial V}{\partial z} = Q(z) + \gamma\sqrt{\epsilon}(V + v/\sqrt{\epsilon}) + \frac{\mu}{\epsilon^{3/2}}\frac{\partial^2 V}{\partial z^2}. \tag{39}$$

Considering here ϵ and μ as small parameters and neglecting the viscous term in the region of packet localization ($z \sim 1$) we obtain the following expansion of V in the parameter $\sqrt{\epsilon}$:

$$V = V_0 + \frac{\gamma\sqrt{\epsilon}}{V_0}\int_0^z [V_0(z') + v/\sqrt{\epsilon}]dz', \tag{40}$$

where the zeroth-order solution $V_0\,(z)$ is given by the following expression:

$$V_0 = \sqrt{2}\sqrt{\int_0^z Q\,(z')\,dz'}. \tag{41}$$

We have assumed that $Q\,(0) = 0,\ \ Q'\,(0) > 0$, and the branch of the square root in the last equation is chosen such that $V_0\,(-z) = -V_0\,(z)\,,\ z \to 0$.

The solution given by Equation (40) is valid in the region of packet localization and we need to match this solution with a solution that describes the shock structure. To obtain an expansion for the latter solution we rescale the variables in Equation (38) as follows: $w = U/\sqrt{\mu\gamma}$, $\eta = \sqrt{\gamma/\mu}\,y$, so that the equation for w takes the following form:

$$w\frac{\partial w}{\partial\eta} = w + \frac{\partial^2 w}{\partial\eta^2} + B, \tag{42}$$

where

$$B = \frac{1}{\gamma^{3/2}\sqrt{\mu}} Q(y) + \frac{v}{\sqrt{\mu\gamma}} \simeq + \frac{v}{\sqrt{\mu\gamma}}.$$

In Equation (42) the instability, viscosity, and nonlinearity are all of the same order, while the driver Q is evaluated at $y \gg 1$ for small μ, i.e., Q is neglected according to the above assumption. The constant B in Equation (42) can be treated as a small constant (compared with w) since within the shock transition $U \gg \bar{U} = v$. Therefore, we look for the solution of Equation (42) in the following form:

$$w = w_0 + Bw_1 + \cdots. \tag{43}$$

In fact, for the purpose of determination of the shock coordinate within the driver period, it is sufficient to obtain only w_0 in Equation (43). The equation for w_0 is the same (apart from rescaling) as Equation (28):

$$w_0 \frac{\partial w_0}{\partial \eta} = w_0 + \frac{\partial^2 w_0}{\partial \eta^2}. \tag{44}$$

Thus, we can obtain the exact integral of this equation using Equation (29):

$$\frac{w_0^2}{2} - \frac{\partial w_0}{\partial \eta} - \ln\left(1 - \frac{\partial w_0}{\partial \eta}\right) = \frac{w_{\max}^2}{2}. \tag{45}$$

To match the solution of this equation with the solution valid in the region of the driver, Equation (40), it is sufficient to take a limit in which the logarithmic term is large:

$$\frac{\partial w_0}{\partial \eta} \simeq 1 - \exp\left(\frac{w_0^2 - w_{\max}^2}{2}\right). \tag{46}$$

This representation of the integral, given by Equation (45), is valid to the left from a maximum of w_0, which is identified with the integration constant $w_{\max}$. The shock structure is the same as that considered in the previous section. The specific part of this solution that needs to be matched to the solution given by Equation (40) can be represented as

$$\eta(w_0) - \eta(w_{\max}) = -\frac{1}{w_{\max}} \ln\{-1 + \exp[w_{\max}(w_{\max} - w_0)]\}. \tag{47}$$

To match this solution with the solution in Equation (40) we take the limit $w_{\max}(w_{\max} - w_0) \gg 1$,

$$w_0 \approx \eta + w_{\max} - \eta_{\max},$$

with $\eta_{\max} \approx \eta(w_{\max})$. Returning to the original variables U and y, we obtain

$$U \approx \gamma(y - y_{\max}) + U_{\max};$$

see Figure 3. The matching procedure leads to the following simple relation between the constant $V_{0\infty}$, the maximum value of $U = U_{\max} = \sqrt{\mu\gamma} w_{\max} \approx U(y_{sh})$ and $y_{sh} \approx \sqrt{\mu/\gamma}\,\eta_{\max}$:

$$U_{\max} - \gamma y_{sh} = \sqrt{\epsilon} V_{0\infty}. \tag{48}$$

To relate the shocktrain parameters $U_{\max}$ and y_{sh}, the following consideration is useful. First, recall that a period averaged $\bar{U} = -v$. Next, we have chosen the packet localization so that $Q(0) = 0$ and we can assume for simplicity that the driver is antisymmetric, $Q(-y) = -Q(y)$. Note that this condition is not really a restricting one, since it can be relaxed by repeating the above expansion of the solution for $y < 0$. The requirement $\bar{U} = -v$, however, yields

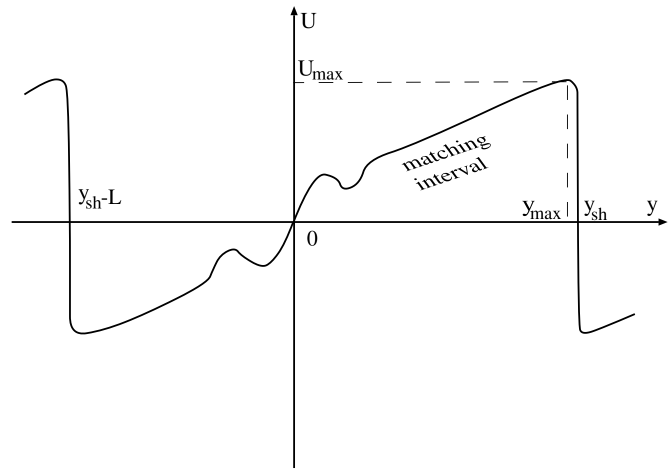

Figure 3. Schematic of matching procedure of the shock and wave packet portions of the solution of Equation (39). One period (of length L) of the solution is shown. The matching is performed in an overlapping region between the region of the wave packet localization, Equation (40), and shock solution, Equation (46). Both asymptotic expressions are valid in this portion of the entire wave profile which changes approximately linearly with coordinate there.

$$\gamma(y_{sh} - L/2) = -v - \sqrt{\epsilon} V_{0\infty},$$

where we have neglected small terms $\sim v^2$. The last equation reflects the asymmetry of the shocktrain $U(y)$ with respect to the point $y = 0$, i.e., $y_{sh} \neq \pm L/2$. This asymmetry is caused by the fact that $\bar{U} = -v \neq 0$. Therefore, the full solution acquires the constant v. The $V_{0\infty}$-term is obviously due to the wave packet. The most important aspect of this solution, however, is that its period is determined by the period of the driver. In a real physical situation the sequence of the wave packets is not strictly periodic and we can only specify a characteristic length scale L instead of the period. At the same time this scale will prescribe the shock spacing, i.e., the minimum wavenumber. This part of the turbulent spectrum is very important for particle acceleration since it is responsible for the confinement of the highest energy particles.

5. NUMERICAL SHOCKTRAIN SOLUTIONS

The purpose of this section is twofold. First, we demonstrate that the traveling wave solutions obtained in the last two sections indeed attract time-dependent solutions of the evolution equations given by Equations (27) and (38), i.e., by the unforced and forced Burgers equations, respectively. Second, we investigate the dynamics of the system as it approaches the attractors. The dynamics includes the unstable wave growth out of a seed perturbation, the shock formation, and shock merging.

We integrate Equation (27) in time. As we emphasized earlier, the initial density perturbation is caused by the cyclotron instability of the CRs in the precursor. However, almost independent of the initial conditions, the undriven system approaches a time asymptotic solution that is exactly the traveling wave solution given by Equation (29). Its period equals the integration box size unless special initial conditions are chosen, such as those lacking all the odd harmonics. Then, the period is naturally a half of the box size. The evolution of the system goes invariably through the coalescence of smaller shocks into larger ones. If the

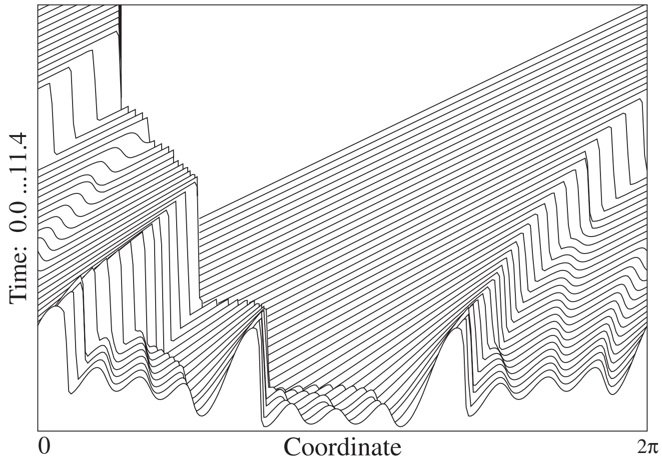

Figure 4. Stack plot of a wave profile evolving in time. The initial profile is a wave packet formed by a superposition of a few modes which model the result of the cyclotron instability of the MHD waves with a compressible component. This initial condition is subjected to the evolution Equation (27) with the following parameters: $\mu = 0.002$, $\gamma = 0.4$. The final wave profile is 2π-periodic and steady (it is shown in a moving reference frame for clarity). One strong shock per period with a linear behavior outside of the shock transition is a strong and stable attractor of this system, exactly coinciding with the analytic solution described in Section 4.

initial amplitude is large enough to make the nonlinearity strong, the shocks arise immediately from any given density profile by steepening. Otherwise, the initial profile growth linearly with the timescale $\sim 1/\gamma$ and then breaks into shocks which merge later in the both cases.

A typical example of such development is shown in Figure 4. Initially, three relatively weak shocks per box are formed with nearly linear waves between them. Then, the shocks move toward each other (in fact a stronger, faster shock overtakes and swallows a weaker and slower one, as usual in Burgers turbulence). In the mean time, the small amplitude waves in-between also steepen somewhat, but their steepening is clearly limited by viscosity. They too are absorbed by stronger shocks. Finally, when only two strong shocks remain after the first big merging, the strongest shock absorbs the weaker one and only one shock per period remains. The overall solution is exactly the piecewise linear "sawtooth" solution given by Equations (34) and (36).

Let us turn now to the situation in which the Drury's instability is accompanied by the cyclotron instability. This case is described by Equation (38). As we noted, the cyclotron instability is assumed to operate in a finite wave band with characteristic wavelength equal to the typical Larmor radius of energetic particles. As an initial condition, we take a wave packet formed by a few unstable harmonics. Having arisen from the cyclotron instability, they are converted by the wave refraction (Kotelnikov et al. 1991) into a wave packet of the density perturbations. Since this process should continue while the Drury's instability develops, the evolution equation in Equation (38) is supplemented by the driving term Q.

The initial condition consists of two linear wave packets per periodic box, so that it takes a few inverse growth rates $1/\gamma$ before the waves in the packets start to steepen and form shocks, Figure 5. Again, relatively weak initial shocks merge to form stronger shocks. However, contrary to the previous case of $Q \equiv 0$, this process does not continue until a single shock with the largest amplitude possible remains. Instead, after two strong shocks are formed by merging of the weak shocks on the

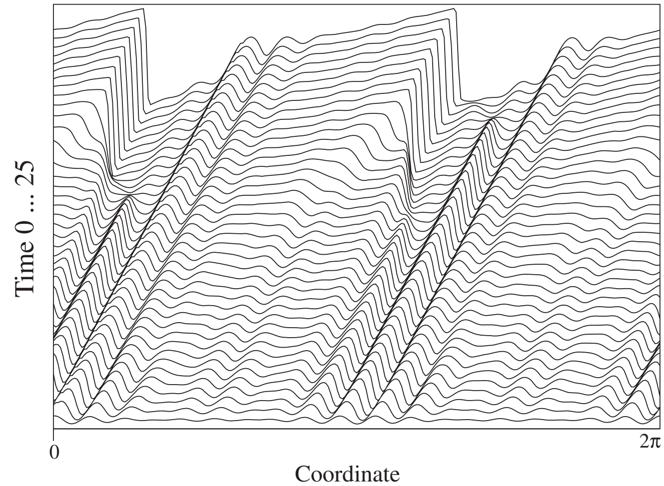

Figure 5. Same as in Figure 4 except the system is driven by three harmonics with the wavenumbers $k = 15, 17, 19$. Without the action of the Drury's instability this driver leads to the formation of two wave packets per period. The stack plot shows the dynamics of the Drury's instability and the final state (see text).

left flanks of the wave packets, the somewhat steepened right flanks actually separate the shocks and prevent them from further merging. This time asymptotic state of the system, Figure 5, was obtained analytically in the preceding section.

6. DISCUSSION AND CONCLUSIONS

Many discussions of the SNR–CR link have been focused on the difficulties of the DSA mechanism to reach the energies inferred from the observations. Still in the wake of the pessimistic Lagage & Cesarsky (1983) estimates, various authors have attempted to demonstrate the ability of an SNR to accelerate particles to the knee ($\sim 10^{15}$ eV) energy and beyond. The most radical suggestion was due to Bell & Lucek (2001) and Bell (2004). It invokes the free energy of already accelerated CRs to drive MHD waves in the CR shock precursor, to levels way above what then was a community paradigm level, i.e., $\delta B \sim B_0$. The latter level is indeed negligible compared to the available shock mechanical energy (and thus CR energy, if acceleration is efficient). The Bell & Lucek idea is appealing in that it seems to have the potential to extend the maximum energy of particles, accelerated by a young SN (particularly if exploded in a progenitor wind) up to the CR ankle ($\sim 10^{18}$ eV). However, the instability saturation mechanism (Bell 2004) considered is the increase in magnetic tension, and so imposes only an *upper bound* on the maximum amplitude. Other standard saturation mechanisms likely to yield lower amplitudes, such as particle trapping, transit time or nonlinear Landau damping and wave steepening (considered in this paper), were not addressed. An equally important problem is that the (fire-hose) instability, studied by Bell (2004), has its maximum growth rate at wavelengths three orders of magnitude shorter than the smallest gyroradius of the CRs that drive this instability. Therefore, these waves are useless for the confinement of the highest energy particles, unless the field amplification is so strong that the particle gyroradius becomes smaller than the wavelength. In the latter case, however, the assumptions under which the instability growth rate is derived would be violated. The impact of the strongly unstable short waves on the slowly growing long waves, that are potentially useful for particle confinement, is unknown. Note that other detailed DSA related studies of the same instability for different sets of parameters but with similar results can be found in Achterberg (1983) and Shapiro et al. (1998).

An important difference between the fire-hose or ion-cyclotron kinetic instabilities and the acoustic (Drury) instability considered in this paper is that the growth rate of the acoustic instability, Equation (25), is almost independent of the wavenumber (see, however, Equation (A6)). The acoustic instability is more robust in that it is hydrodynamic in nature and cannot be stabilized by kinetic (e.g., quasilinear) effects such as the isotropization of particle distribution or particle trapping (Achterberg & Blandford 1986). Moreover, the magnetic shocktrain structures efficiently trap and mirror energetic particles (Malkov & Diamond 2006). Usually, these processes quickly isotropize the energetic particle distribution, thus modifying and suppressing the growth rates of the cyclotron and fire-hose unstable Alfvén waves. It is also important to note that shock merging in the Burgers model naturally generates longer scales which is not only crucial for the confinement of the highest energy particles but also prevents the magnetic energy being damped rapidly (Diamond & Malkov 2007).

It follows that the mechanism of transforming turbulent magnetic energy toward long scales comes in two flavors. First, shocktrains generated after the onset of the Drury's instability provide an efficient scattering environment for MHD waves generated by the ion-cyclotron unstable accelerated particles (Diamond & Malkov 2007). The scattering of these waves in wavenumber generates longer scales (along with shorter ones). The specification of the scattering environment for further application to the inverse cascade theory developed in the above paper was one of the main goals of the present paper. Second, shocks coalesce within a shocktrain and generate longer scales and stronger shocks in the CR shock precursor. The latter process is generic to the Burgers turbulence both in a decay (undriven) regime (Gurbatov et al. 1992) and in the case of a stochastic (Chekhlov & Yakhot 1995) or deterministic driver (Malkov et al. 1995).

The situation considered in this paper is different from the conventional Burgers turbulence in two ways. First, the Drury's instability generates all harmonics at the same rate so that there is no preferred scale and the shocks merge till a system-wide scale (e.g., the longest harmonic in a simulation) is reached. In the context of the CR shock precursor, of course, the shock merging process is always limited by the precursor crossing time, $\tau_c = L_p/u_{\rm sh}$. Nevertheless, a number of relatively strong shocks (about 5–10 on average) may be present in the shock precursor at any moment of time while they are continuously formed and merge. Under these circumstances, the acceleration will likely proceed at a faster than Bohm rate (Malkov & Diamond 2006). Second, if the ion-cyclotron instability of accelerated particles also disturbs the plasma density (as discussed in Section 4), a driving term appears on the rhs of the Burgers equation. The result is different from the previous case in that the shock merging process is limited by the longest distance between the shocks prescribed by the period of the driver, i.e., by the distance between the wave packets generated by the cyclotron instability. In fact, this process is favorable for acceleration, since scales that are significantly longer than the proton gyroradius (beat-wave length of the cyclotron instability rather than the proton gyroradius) are created. Therefore, almost independent of the cyclotron instability, the acoustic instability creates a more efficient scattering environment which substantially improves particle confinement and enhances particle acceleration, as was shown in Malkov & Diamond (2006). This process will be studied in more detail in a future publication.

The final note to make is about limitations of a formally hydrodynamic (nonmagnetic) treatment of the acoustic instability pursued in this paper. This approach was chosen primarily for simplicity and clarity. The Burgers equation can be easily generalized to one of its "magnetic" versions, the most generic of which is the so-called derivative nonlinear Schrödinger equation, DNLS. However, as long as magnetic field is weak, as already discussed in Section 1, its dynamical role can be ignored and the Burgers model is sufficient to adequately describe the emerging scattering environment that is responsible for confinement and acceleration of energetic particles.

Support by NASA under grants NNG 04GK96G and NNX 07AG83G and by the Department of Energy, grant no. DE-FG02-04ER54738, is gratefully acknowledged.

APPENDIX

Here, we perform a standard linear stability analysis of the system given by Equations (1)–(4). The difference between the dispersion relation obtained below and those obtained in the preceding studies (Zank et al. 1993; Finazzi & Vietri 2008) is in the choice of the equilibrium CR distribution F_0 in general, as discussed in Section 2.2, and in the inclusion of the CR pressure gradient in particular. This gradient alone produces unstable solutions, not found in the above papers. Conversely, the "squeezing" instability found by Zank et al. (1993) is not present here because of a different treatment of the connection region between the CR and thermal plasma. As we mentioned, there is a distinctive gap between the two distributions ahead of the subshock. Therefore, the CR distribution function tends to zero also at lower momenta. Note that the treatment of the squeezing instability in Zank et al. (1993) does not specifically address the modified CR shock precursor.

We start from a standard WKB Ansatz (though a local approximation is sufficient for $kL_p \gg 1$) applied to Equations (1) and (2):

$$\tilde{u} = \sum_k u_k e^{ikx - i\omega t}$$

and similar expansions of $\tilde{P}_c$, $\tilde{\rho}$, and $\tilde{P}_g$ will be used. A simple algebra leads to the following linear dispersion equation:

$$\left(\omega' - iu_{0x}\right)^2 - k^2 c_s^2 - \frac{ik}{\rho_0}\bar{P}_{cx} = \left(\omega' - iu_{0x}\right)\frac{k}{\rho_0}\frac{P_{ck}}{u_k}. \quad \text{(A1)}$$

Here index x stands for the x-derivatives of the background variables u_0 and $\bar{P}_c$. We have retained only leading in $M_s^{-1} \ll 1$ terms of this kind and neglected the viscous damping. The CR response on the rhs can be calculated by linearizing Equation (3). To simplify the formalism, we restrict our treatment to that (largest) part of the CR precursor where $p_{\rm min} > 1$ (the lower momentum cut off is above $p \sim mc$ in dimensional variables, see Section 2.2). Then, using Equation (3) for P_{ck} we obtain

$$\frac{P_{ck}}{u_k} = \frac{4\pi}{9}kmc^2 \int_0^\infty \frac{p^3 F_0(p,x)}{(\omega' + i\kappa k^2)^2} \times \left[4\omega' + 3i\kappa k^2 - \frac{i}{3}u_{0x}\frac{16\omega'^2 + 19i\omega'\kappa k^2 - 6\kappa^2 k^4}{(\omega' + i\kappa k^2)^2}\right] dp. \quad \text{(A2)}$$

Here F_0 is given by Equation (19) which allowed us to extend the integration limits to $(0, \infty)$, essentially on the same grounds as those discussed in the paragraph following Equation (20). However, since $\omega' \neq 0$ here, an additional restriction on $p_* (x)$ should be imposed to avoid the necessity of cutting the integral from above:

$$\frac{\omega'}{k^2} \ll \kappa (p_*) . \quad \text{(A3)}$$

This condition can be translated into the following one, $kL_p \gg M_s^{-1}$, which should of course be always fulfilled, given the local treatment of the dispersion equation. The latter condition is a softened version of the adiabaticity condition $k\kappa (p) \gg c_s$ discussed in Sec.(2.2). For verification purposes, we first consider an opposite case of very long waves, when the condition in Equation (A3) is not met. The spectrum must be cut from above or becomes converging by itself due to a change of the confinement regime as we discussed earlier. To be consistent, we should drop the u_{0x} and $\bar{P}_{cx}$ terms in Equations (A1) and (A2) for such long waves, assuming that the background plasma is homogeneous. Then, Equation (A2) can be written as

$$\frac{P_{ck}}{u_k} = \frac{4}{3} \frac{k}{\omega'} \bar{P}_c . \quad \text{(A4)}$$

Clearly, the factor 4/3 should be identified with γ_c, the CR adiabatic index, since the contribution to the CR pressure comes from ultrarelativistic particles. Then, from Equation (A1) we obtain the well known result found by Ptuskin (1981):

$$\omega'^2 = k^2 \left(c_s^2 + \gamma_c \bar{P}_c / \rho_0 \right) . \quad \text{(A5)}$$

In this paper we are interested in an opposite case, characterized by Equation (A3). Assuming in addition that the acceleration is efficient, at least to the extent that

$$\frac{P_c}{\rho u^2} > \frac{1}{M_s},$$

we can discard u_{0x} in Equation (A1):

$$\omega'^2 - k^2 c_s^2 - \frac{ik}{\rho_0} \bar{P}_{cx} = \frac{4\pi}{9} \omega' \frac{1}{\rho_0} mc^2 k^2 \times \int_0^\infty \frac{p^3 F_0 (p, x)}{(\omega' + i\kappa k^2)^2} [4\omega' + 3i\kappa k^2] dp .$$

Expanding the integrand in small $\omega'/\kappa k^2$ we obtain the following dispersion equation

$$\left(1 - \frac{k_0^2}{k^2}\right) \omega'^2 - k^2 c_s^2 = \frac{ik}{\rho_0} \bar{P}_{cx} - i\Omega\omega' , \quad \text{(A6)}$$

where we denoted

$$\Omega = \frac{n_c}{3n_0} \frac{c^2}{\kappa_*} p_* , \quad k_0^2 = \frac{\Omega}{q \left| \phi_0 \right|} .$$

Here $\langle \cdot \rangle$ denotes the momentum average, and $n_c (x)$ is the CR number density ahead of the subshock.

REFERENCES

Achterberg, A. 1981, A&A, 98, 195
Achterberg, A. 1983, A&A, 119, 274
Achterberg, A., & Blandford, R. D. 1986, MNRAS, 218, 551
Aharonian, F., Buckley, J., Kifune, T., & Sinnis, G. 2008, Rep. Prog. Phys., 71, 096901
Bell, A. R. 2004, MNRAS, 353, 550
Bell, A. R., & Lucek, S. G. 2001, MNRAS, 321, 433
Berezhko, E. G., & Völk, H. J. 2004, A&A, 419, L27
Blandford, R. D. 1980, ApJ, 238, 410
Blandford, R., & Funk, S. 2007, in AIP Conf. Ser. 921, The First GLAST Symposium, ed. S. Ritz, P. Michelson, & C. A. Meegan (Melville, NY: AIP), 62
Blasi, P., Gabici, S., & Vannoni, G. 2005, MNRAS, 361, 907
Chekhlov, A., & Yakhot, V. 1995, Phys. Rev. E, 51, R2739
Diamond, P. H., & Malkov, M. A. 2007, ApJ, 654, 252
Drury, L. O., & Falle, S. A. E. G. 1986, MNRAS, 223, 353
Ellison, D. C., Berezhko, E. G., & Baring, M. G. 2000, ApJ, 540, 292
Finazzi, S., & Vietri, M. 2008, ApJ, 687, 287
Gurbatov, S. N., Malakhov, A. N., & Saichev, A. I. 1992, Nonlinear Random Waves and Turbulence in Nondispersive Media (Nonlinear Science: Theory & Applications) (New York: Wiley)
Kang, H., Jones, T. W., & Ryu, D. 1992, ApJ, 385, 193
Kennel, C. F., Edmiston, J. P., & Hada, T. 1985, Geophysical Monograph Series 34 (Washington, DC: American Geophysical Union), 1
Kotelnikov, A. D., Polyudov, A. N., Malkov, M. A., Sagdeev, R. Z., & Shapiro, V. D. 1991, A&A, 243, 546
Lagage, P. O., & Cesarsky, C. J. 1983, A&A, 125, 249
Landau, L. D., & Lifshitz, E. M. 1987, Fluid Mechanics (Oxford: Pergamon)
Malkov, M. A. 1996, Physica D, 95, 62
Malkov, M. A. 1997a, ApJ, 485, 638
Malkov, M. A. 1997b, ApJ, 491, 584
Malkov, M. A., & Diamond, P. H. 2006, ApJ, 642, 244
Malkov, M. A., & Drury, L. O. 2001, Rep. Prog. Phys., 64, 429
Malkov, M., Kotelnikov, A., & Kennel, C. 1995, Physica D, 86, 480
Moskalenko, I. V., Porter, T. A., Malkov, M. A., & Diamond, P. H. 2007, arXiv:0705.3854
Papadopoulos, K. 1985, Geophysical Monograph Series 34 (Washington, DC: American Geophysical Union), 59
Pohl, M., Yan, H., & Lazarian, A. 2005, ApJ, 626, L101
Ptuskin, V. S. 1981, Ap&SS, 76, 265
Sagdeev, R. Z. 1979, Rev. Mod. Phys., 51, 11
Shapiro, V. D., Quest, K. B., & Okolicsanyi, M. 1998, Geophys. Res. Lett., 25, 845
Skilling, J. 1975, MNRAS, 173, 255
Uchiyama, Y., Aharonian, F. A., Tanaka, T., Takahashi, T., & Maeda, Y. 2007, Nature, 449, 576
Vink, J., & Laming, J. M. 2003, ApJ, 584, 758
Vladimirov, A., Ellison, D. C., & Bykov, A. 2006, ApJ, 652, 1246
Zank, G. P., Axford, W. I., & McKenzie, J. F. 1990, A&A, 233, 275
Zank, G. P., Webb, G. M., & Donohue, D. J. 1993, ApJ, 406, 67
Zirakashvili, V. N., Ptuskin, V. S., & Völk, H. J. 2008, ApJ, 678, 255